Stretching and breaking duplex DNA by chemical force microscopy

Aleksandr Noy[1], Dmitri V Vezenov[1], Jon F Kayyem[2,3], Thomas J Meade[2] and Charles M Lieber[1]

Background: Specific interactions between complementary strands of DNA and other molecules are central to the storage, retrieval and modification of information in biological systems. Although in many cases the basic structures of duplex DNA and the binding energetics have been well characterized, little information is available about the forces in these systems. These forces are of critical importance because they must be overcome, for example, by protein machines during transcription and repair. Recent developments in atomic force microscopy make possible direct measurements of such forces between the individual oligonucleotide strands that form DNA duplexes.

Results: We used the chemical force microscopy technique, in which oligonucleotides are covalently linked to the force microscope probe tip and the sample surface, to measure the elongation and binding forces of individual DNA duplexes. The separation forces between complementary oligonucleotide strands were found to be significantly larger than the forces measured between noncomplementary strands, and to be consistent with the unbinding of a single DNA duplex. With increasing applied force, the separation of complementary strands proceeded in a stepwise manner: B-form DNA was stretched, then structurally transformed to a stable form of DNA approximately twice the length of the B form, and finally separated into single-stranded oligonucleotides. These data provide a direct measurement of the forces required to elastically deform and separate double-stranded DNA into single strands.

Conclusions: Force microscopy provides a direct and quantitative measurement of the forces and energetics required to stretch and unbind DNA duplexes. Because the measurements can be carried out readily on synthetic oligonucleotides and in the presence of exogenous molecules, this method affords an opportunity for directly assessing the energetics of distorting and unbinding specific DNA sequences and DNA complexes. Such data could provide unique insights into the mechanistic steps following sequence-specific recognition by, for example, DNA repair and transcription factors.

Addresses: [1]Department of Chemistry and Chemical Biology, Harvard University, 12 Oxford Street, Cambridge, MA 02138, USA. [2]Division of Biology and the Beckman Institute, California Institute of Technology, Pasadena, CA 91125, USA. [3]Clinical Micro Sensors, 101 Waverly Drive, Pasadena, CA 91105, USA.

Correspondence: CM Lieber and TJ Meade
E-mail: cml@cmliris.harvard.edu and tmeade@druggist.gg.caltech.edu

Keywords: binding forces, chemical force microscopy, DNA, structural transition

Received: **21 May 1997**
Revisions requested: **16 June 1997**
Revisions received: **24 June 1997**
Accepted: **25 June 1997**

Chemistry & Biology July 1997, 4:519–527
http://biomednet.com/elecref/1074552100400519

Introduction

Highly specific interaction forces in double-stranded DNA play a well-known role in the storage and retrieval of genetic information [1]. Furthermore, these forces determine the elastic properties of duplex DNA that are believed to be important for its packaging in the nucleus, for cell division, and for many of the interactions with proteins, for example during transcription and repair [2–5]. Much of our knowledge of these critical forces comes indirectly from measurements of binding energetics, which can be determined by affinity [6], melting [7,8], calorimetry [9] and structural studies [10]. Recent technological advances are now enabling the direct assessment of interaction and deformation forces at the single molecule level in DNA and other biological molecules [11–15]. For example, after chemically linking micrometer-size beads to the ends of single-stranded and double-stranded DNA, it has been possible to measure directly the forces required to stretch the polynucleotides using magnetic, optical and other means to pull on the bead [13,16]. This work has provided new experimental insights into the entropic elasticity of polymers in general [17,18], and the observation of a highly stretched form of duplex DNA [12,13]. The need to use relatively large micrometer-size beads as handles in these experiments does, however, mean that long, kilobase, single-stranded and double-stranded DNA molecules must be used for such studies. It has not, therefore, been possible to assess specific chemical contributions to the stretching and binding forces in DNA. Because stretching induced by proteins *in vivo* is typically confined to relatively short DNA stretches, it is especially important to elucidate these molecular-level contributions.

Atomic force microscopy [19–21] represents an alternative approach for probing binding and stretching forces on a

Figure 1

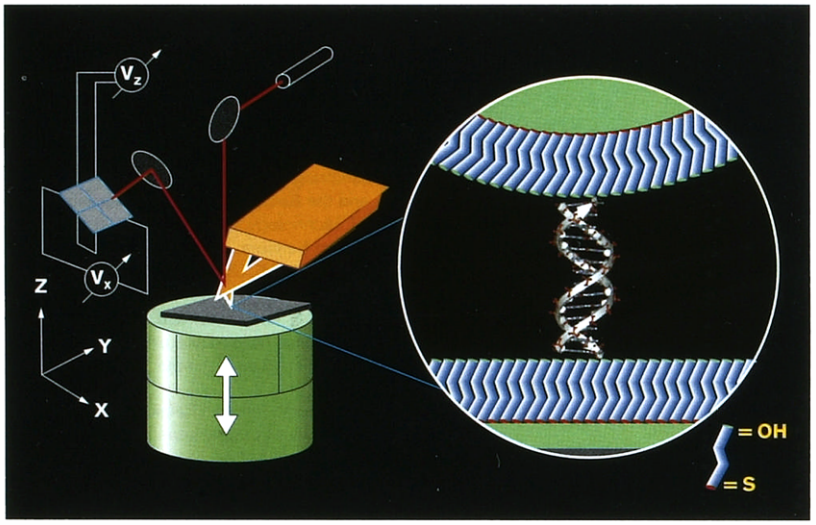

A schematic illustration of the chemical force microscopy setup. The sample is mounted on a piezoceramic transducer (green) that can move the sample vertically with subangstrom precision. The probe tip is attached to a flexible cantilever (yellow) and the laser beam (red) is reflected off the cantilever back onto a photodiode to monitor cantilever deflection. The inset shows a cartoon representation of interactions between two complementary strands immobilized on the tip and sample surfaces. Both the tip and the sample are coated with gold; self-assembled monolayers of alkanethiols (blue) are then formed on the gold surface. The DNA shown in the inset corresponds to the relaxed B-DNA conformation.

molecular scale. In the atomic force microscopy experiment, force is measured by monitoring the deflection of a flexible cantilever spring that terminates in a sharp tip, while the probe–sample distance is controlled by means of a piezoelectric scanner (Figure 1). To determine binding and/or stretching forces then requires a means of attaching the system of interest between the tip and substrate. Nonspecific adsorption of biotinylated bovine serum albumin was used for surface modification in experiments measuring binding interactions between biotin and streptavidin [14, 22,23]. In addition, atomic force microscopy has recently been used to measure duplex DNA binding forces by covalently attaching complementary oligonucleotides to reactive siloxane layers deposited on tips and substrates [24]. While this work has been important in demonstrating the ability to measure duplex-binding forces with atomic force microscopy, we believe that the attachment chemistry has several limitations. First, siloxane layers made using short-chain silanes exhibit considerable disorder and are not bonded to the substrate and tip at every silicon lattice site [25]. This can lead to considerable uncertainty and variation in the elastic properties of the attachment and so complicate the analysis of DNA stretching. Second, subsequent reactions with the surface of the siloxane layer allow little control of the surface density and the arrangement of oligonucleotides. Consequently, only ~3% of the linked oligonucleotides were found to form duplexes [24].

Here, we have investigated both binding and stretching forces in duplex DNA using an approach based on our previous chemical force microscopy studies [26–28]. Chemical force microscopy employs covalent functionalization of gold-coated probe tips and substrates with crystalline self-assembled monolayers (SAMs) of alkanethiols [29] (Figures 1,2b). Alkanethiol SAMs provide a flexible and robust system for tailoring the molecular properties of surfaces [30–32], and together with chemical force microscopy they have been used to quantify intermolecular forces between neutral and charged surfaces in aqueous and organic media [27,28]. To study intermolecular forces in duplex DNA, we prepared mixed alkanethiol-based SAMs consisting of hydroxyl-terminated hexadecanethiol and oligonucleotide-terminated hexadecanethiol on probe tips and substrates. Both complementary and noncomplementary oligonucleotide interactions were investigated, in order to assess unambiguously the binding forces of single duplex structures. In addition, the well-defined and rigid SAM structure enabled the determination of the stretching behavior of individual oligonucleotide duplexes and thus the elucidation of the pathway by which unbinding occurs.

Results and discussion

DNA immobilization

Two complementary DNA 14-mers, 5′-TCGGACAATG-CAGA-3′ (LT) and 5′-TCTGCATTGTCCGA-3′ (LS), with covalently tethered hexadecanethiol linkers were prepared as outlined in Figure 2a. The sequences were designed such that any shift of one strand in the duplex with respect to another would allow the formation of at most two Watson–Crick base pairs, thus ensuring an 'all-or-none' type of binding. Melting/annealing cycles carried out on solutions of the LT–LS pair exhibited no hysteresis and were therefore consistent with an all-or-none binding behavior.

Mixed monolayers consisting of either LT or LS alkanethiol-linked oligomers and a 16-thiohexadecanol spacer were formed on gold-coated Si_3N_4 probes and gold-coated

Figure 2

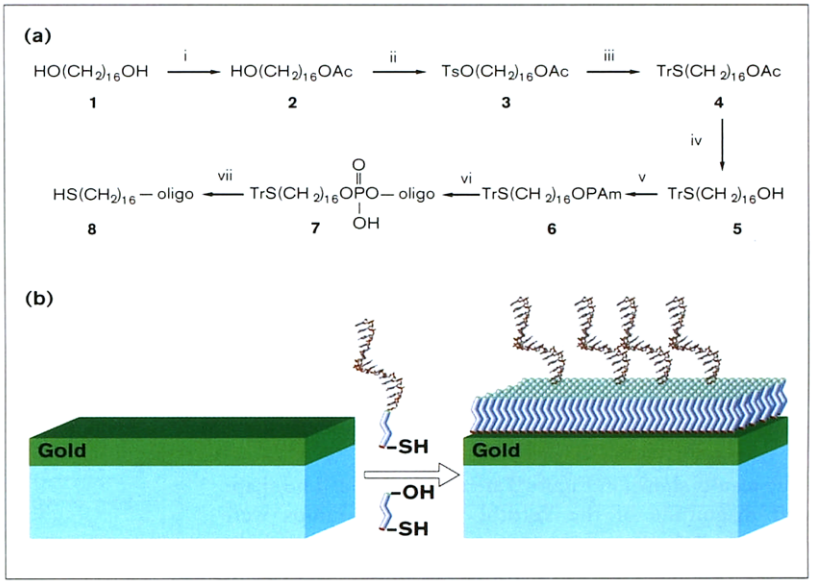

Preparation of surface-immobilized oligonucleotides. **(a)** A synthetic route to the 5′-alkylthiol oligonucleotide conjugate **8**. Ac = $COCH_3$, Ts = 4-$CH_3C_6H_4SO_2$, Tr = $(C_6H_5)_3C$, PAm = $P(OCH_2CH_2CN)(N(CH(CH_3)_2)_2)$. Reaction conditions: i, acetic anhydride, 4-dimethylaminopyridine (DMAP), CH_2Cl_2; ii, dry pyridine, *p*-TsCl; iii, triphenylmethyl mercaptan (TPMM), N,N′-dimethylformamide (DMF); iv, NaOH, CH_3OH; v, 2-cyanoethyl diisopropylchlorophosphoramidate, N,N-diisopropylethylamine (DIEA), CH_2Cl_2; vi, automated oligonucleotide synthesis, vii, isolation and purification by reverse phase HPLC. Each intermediate was purified by flash chromatography. **(b)** A schematic illustrating monolayer formation and surface immobilization of the oligonucleotides prepared as shown in (b). Mixed monolayers of 16-thiohexadecanol and hexadecanethiol functionalized with oligonucleotides were formed by spontaneous self-assembly from 3:1 H_2O:EtOH solutions. The resulting hydroxyl-terminated monolayer has a hydrophilic surface from which the DNA strands protrude.

single-crystal silicon substrates by simultaneous adsorption of the two thiols (Figure 2b). Because both the LT/LS thiol linker and the 16-thiohexadecanol were of identical length, the linker was completely embedded in the monolayer and only the oligonucleotide protruded from the hydrophilic hydroxyl-terminated surface. The ratio of solution concentrations of the two thiols was chosen so as to dilute significantly the surface density of immobilized DNA. An oligonucleotide surface density of 0.05 strands/nm^2, corresponding to a nearest neighbor distance of 4.5 nm, was estimated from scanning tunneling microscopy images. When compared to the molecular cross section of LT and LS oligonucleotides, this surface density was sufficiently low to ensure that interchain interactions between like oligomers on either the substrate or the tip surfaces did not contribute significantly to measurements of LT–LS intermolecular forces.

The binding competence of the surface-bound oligonucleotides was confirmed by hybridization with ^{32}P-labeled and fluorescein-labeled complementary and noncomplementary oligonucleotides. We found that samples hybridized with the complementary ^{32}P-labeled oligonucleotide exhibited more than ten times higher activity levels (853 counts/min) than samples hybridized with the noncomplementary oligonucleotide (84 counts/min). The activity exhibited when binding the complementary oligonucleotide could also be eliminated by varying the solution ionic strength or temperature to regimes that preclude duplex formation in homogenous solution. In addition, gold surfaces coated with only the 16-thiohexadecanol monolayer and hybridized with ^{32}P-labeled LS or LT did not show significant counts above background activity. Similar results were also obtained when imaging surfaces hybridized with complementary and noncomplementary fluorescein-labeled oligonucleotides using confocal fluorescence microscopy. These results demonstrate that our surface-bound LT and LS oligonucleotides can produce sequence-specific duplex DNA structures similar to those observed in solution.

Force versus distance measurements

The intermolecular forces between probe tips and substrates functionalized with different combinations of the LT and LS oligonucleotides were determined from force versus displacement curves. To obtain these curves, the scanner of the force microscope was used to translate with angstrom-level control the oligonucleotide-functionalized substrates into and out of contact with an oligonucleotide-functionalized tip mounted on the cantilever (Figure 1). The cantilever deflection was monitored during the approach/withdrawal cycle using a photodetector sensitive to changes in the position of the laser beam that was reflected from the back of the cantilever. The cantilever force constant, which was determined directly for these experiments [33], was then used to convert the measured deflection into a force. Hysteresis between the approach and the withdrawal parts of the curve (as seen in Figure 3) reflects the binding interaction between the tip and substrate surfaces. The vertical jump that occurs along the withdrawal part of the curve corresponds to the point at which the cantilever restoring force just exceeds the intermolecular binding force between the oligonucleotides on the tip and substrate. It therefore marks the point at which the oligonucleotides separate completely. The magnitude

of this vertical jump can be associated with a binding/unbinding force.

Representative force versus displacement curves obtained for interactions between complementary (LT–LS) and noncomplementary (LS–LS) oligonucleotides are shown in Figure 3. The relative magnitudes of the binding forces between noncomplementary (trace I) and complementary (trace II) oligonucleotides are consistent with the expected nature of interactions; that is, the complementary interaction exhibits a significantly larger binding force than that observed for the noncomplementary one. In addition, the withdrawal curve for the duplex (Figure 3, trace II) exhibits a highly nonlinear shape, with an intermediate slope prior to unbinding that is indicative of substantial stretching of the DNA. The stretching and binding behavior of complementary oligonucleotide pairs is quantified below.

The results shown in Figure 3 are reproducible. The shape and magnitude of the vertical unbinding jumps were similar both between repeated measurements done at the same sample-surface site and between experiments using samples and pairs of probe tips with differently functionalized oligonucleotides. Typically, at least 150 curves similar to trace II in Figure 3 were obtained for complementary oligonucleotides at the same surface site. Reproducibility in approach and withdrawal curves for complementary oligonucleotides at the same surface site (using the same LT–LS pair) demonstrates that, during our experiments, the LT and LS oligonucleotides remained bound to their linkers and to the tip and sample surfaces. We believe that the reproducibility of these measurements reflects the well-defined nature of the chemistry developed for attaching oligonucleotides to the substrate and tip surfaces and the stability of the alkanethiol monolayers.

To quantify the magnitude and uncertainty of the binding force, multiple force curves were plotted as histograms of the number of times a particular force was observed versus its magnitude (Figure 4). An average adhesion force of 0.10 ± 0.07 nN was obtained for interactions between noncomplementary oligonucleotides (Figure 4a); this corresponds to nonspecific interactions between the surfaces [28]. In contrast, when the complementary LT–LS pair was investigated, at least 10% of the force curves yielded significantly higher adhesion forces with an average of 0.46 ± 0.18 nN (Figure 4b). Occasionally, a bimodal distribution with peaks at 0.45 nN and 0.90 nN was observed (Figure 4c). Because the estimated contact area of the functionalized tip and sample produced 25 or fewer molecular contacts [27], it was possible (based on the observed density of oligonucleotides) to form at most one or two duplexes in our experiments. Hence, we believe that the bimodal distribution is a manifestation of the unbinding of either one (0.45 nN) or two (0.90 nN) LT–LS duplexes.

Figure 3

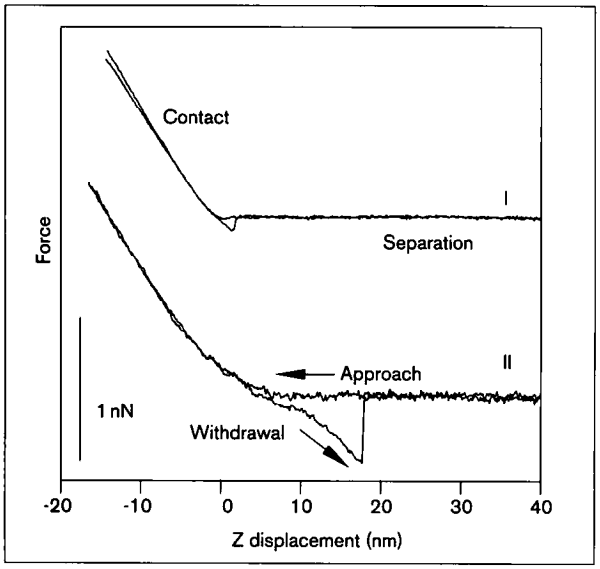

Representative force versus distance curves obtained for tips and samples functionalized with oligonucleotides. Trace I: noncomplementary pair in which the tip and surface were functionalized with LS. Trace II: complementary pair in which the tip was functionalized with LT and the surface was functionalized with LS. The force versus distance curve was obtained by driving the sample into and out of contact with the probe tip while monitoring the cantilever deflection. The tip–sample separation rate was ~60 nm/s in these experiments. Regions of contact and separation are indicated on trace I and the directions of approach and withdrawal are shown on trace II. The hysteresis between the approach and withdrawal parts of the curve is caused by the tip–sample binding interactions.

In addition, the energy required to break the LT–LS duplex was estimated by integrating the force versus distance data. The resulting value of 520 ± 150 kJ/mol (or 37 kJ/mol per base pair) is significantly higher than the 14-mer binding enthalpy value of 310 kJ/mol (22 kJ/mol per base pair) calculated from equilibrium solution denaturation experiments using published procedures [7]. This difference is, however, expected because the force microscopy experiment unbinds the duplex by pulling it from opposite ends and, in doing so, considerable energy is used to stretch the DNA elastically. We believe that probing duplex stretching (and not simply its binding energy) is an important point, because stretching is known to occur upon binding of RecA and other proteins to DNA during transcription and repair [34], and during cell division [3].

DNA stretching

The nonlinear shape of the withdrawal curve for the LT–LS duplex is indicative of mechanical stretching of the duplex prior to unbinding (Figure 3). Other explanations of this behavior, such as mechanical deformation of the monolayer and/or linker, and/or reorientation of the duplex

Figure 4

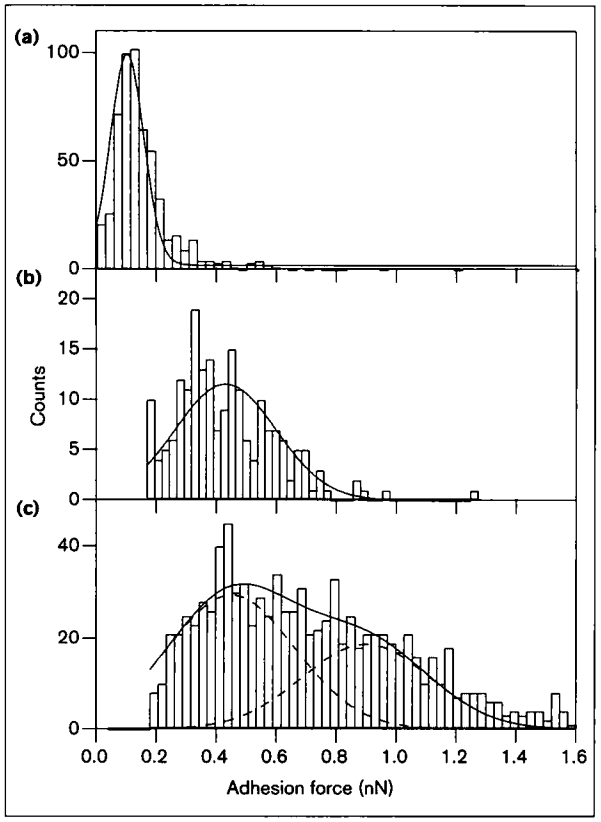

Histograms of the binding force values obtained from multiple measurements between gold surfaces functionalized with the DNA oligonucleotides. **(a)** Noncomplementary pair: tip, LT; sample, LT. **(b)** Complementary pair: tip, LS; sample, LT. **(c)** The distribution for two complementary pairs of strands: tip, LS; sample, LT. Peaks corresponding to noncomplementary interactions (< 150 pN) were removed from (b) and (c) for clarity. Solid lines in (a) and (b) represent best fits to a Gaussian distribution. The solid line in (c) is the best fit to a sum of the two Gaussian distributions indicated by dashed lines.

between the tip and substrate, are very unlikely for the following reasons. First, our previous chemical force microscopy studies of functionalized alkanethiol monolayers never revealed a large range of extension values for small changes of forces as observed in Figure 3 [27,28]. Second, a reorientation of the duplex should require very small forces per distance, in contrast to the experimental data. Hence, we believe that the only consistent explanation for the nonlinear force–displacement data from our experimental system is duplex stretching. The stretching of short oligonucleotide duplexes using the force microscope is a new and central result of our studies.

To obtain a quantitative understanding of the behavior of the DNA under tension, we converted the data into measures of force against separation (the distance between tip

Figure 5

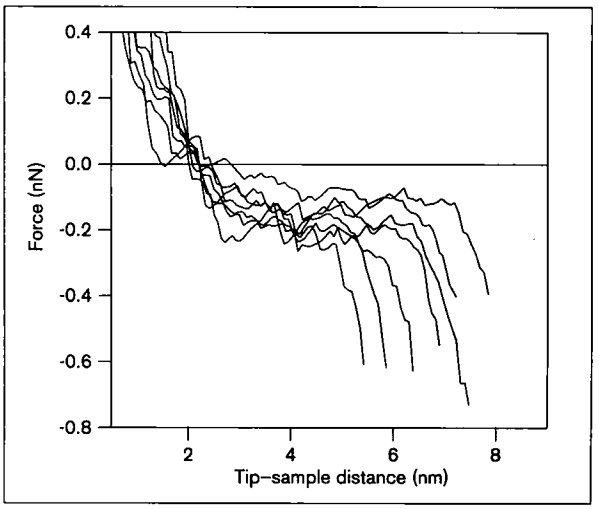

Force versus separation plots obtained from individual approach/withdrawal traces for interactions between complementary DNA strands.

and sample) by deconvoluting the cantilever deflection away from or towards the substrate (Figure 5). These data show that tip–sample repulsive interactions (positive forces) decrease to zero at distances ≥ 2 nm. The zero-force distance corresponds to the tip–substrate separation with the duplex fully extended but not under tension. The zero-force distance varied between 2 nm and 4 nm for individual tips and did not exceed the 4.7 nm length expected for a 14 base pair duplex. The variation in zero-force distance is likely to be due to the oligonucleotide linker being located off the tip apex and/or a misalignment in the contact between the tip-bound and substrate-bound oligonucleotides. These uncertainties do not, however, significantly affect the interpretation of the data.

Separation past the zero-force point put the duplex in tension (negative forces) and produced a curve with a short elastic stretching region, a pronounced flat region where the separation increased rapidly under almost constant force (indicative of a structural transformation), and a relatively stiff elastic region immediately prior to duplex separation. These features, common to the individual experiments, are highlighted in an average plot of individual force versus separation curves (Figure 6). The average curve shows a relatively abrupt transition at a tensile force of 120 ± 50 pN with the DNA duplex length increasing to almost twice its original value before unbinding. The average elongation of the DNA duplex at the unbinding point was 4.6 ± 1.0 nm. This behavior is also consistent with the doubling of the duplex length and, therefore, requires a major structural rearrangement. Structural models for the B-form and the stretched form

Figure 6

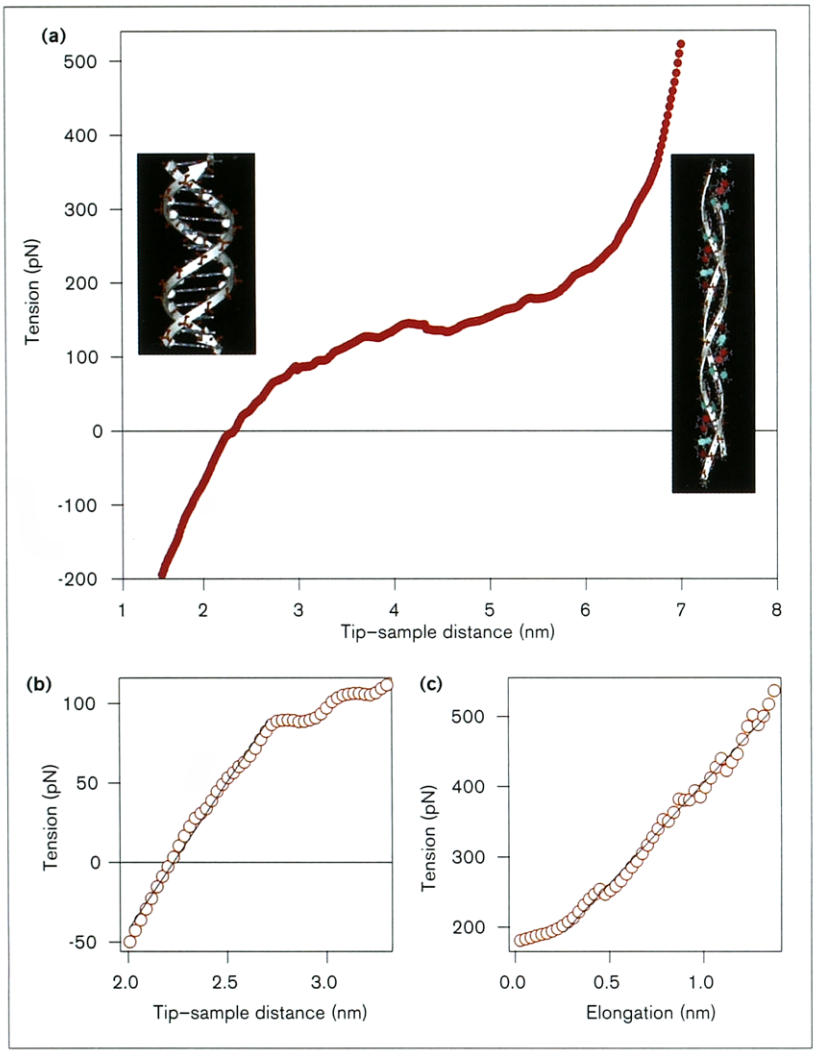

Stretching duplex DNA. **(a)** The average is shown for 20 individual applied force versus tip–sample distance curves obtained for interactions between complementary DNA strands. Data are represented in the form of tension (opposite to applied force) versus tip–sample distance. The common shape is preserved by normalizing the length scale of individual traces to an average tip–sample distance at the point of duplex break up (7.0 ± 0.5 nm). The average curve shows a distinct transition region that can be attributed to a stretching transition. Structural models of B-DNA and S-DNA (stretched DNA) structures are placed next to the corresponding regions of the curve. **(b)** A magnification of the averaged curve immediately before the B-DNA to S-DNA transition. This region was used to calculate the B-DNA elastic modulus. Experimental data, red; linear fit, black. **(c)** The average applied tension versus elongation data corresponding to S-DNA stretching. Experimental data, red; linear fit, black. The curves were shifted relative to each other to match a common transition point, because S-DNA breaks at different points in individual approach/withdrawal cycles; these differences are due to variations in the location of the oligonucleotide linker off the tip apex and/or a misalignment in the contact between the tip-bound and substrate-bound oligonucleotides.

of DNA [35] are indicated at their corresponding locations on the force–distance curve (Figure 6).

Mechanical extension of duplex DNA to 1.7–2 times its natural length has also been observed recently in experiments on micrometer-length pieces (kilobases) of DNA [2,12,13,36,37]. To the best of our knowledge, the present work is the first direct experimental observation of such a structural transition in a short duplex, formed from synthetic oligonucleotides. On the basis of the large change in length at a nearly constant force, it was predicted that stretching induces a cooperative structural transition to a new conformation [2,12,38]. Molecular modeling [12,35] and molecular dynamics simulations [38] have suggested several possible structures (e.g. stretched or S-DNA and a DNA ladder) in which the bases maintain Watson–Crick pairing, but are inclined at an angle such that base–base stacking becomes interstrand rather than intrastrand. The S-DNA structure is shown schematically in Figure 6a.

Overall, our DNA extension versus tension data (e.g. Figure 6) are remarkably similar to the curve calculated by Konrad and Bolonick [38] for stretching a DNA 12-mer. But while their simulation predicts a ladder structure, our experiments cannot distinguish at this stage between ladder and S-DNA structures. The transition threshold force measured by force microscopy, 120 ± 50 pN is in reasonable agreement with the value found by the simulation (85 pN), especially given that another modeling study found a transition threshold at ≥ 140 pN

[35]. Our threshold can also be compared to the measurements on micrometer-length DNA, where a smaller (70 pN) value has been found [12,13]. It is possible that this difference may reflect the gross differences in the lengths (i.e. 14 base pairs compared with thousands of base pairs) of the DNA studied. Despite these uncertainties, we are encouraged about the opportunities for further study, because both the sequence composition and the length of the DNA can be explicitly and systematically controlled in our system.

Finally, our data can be used to determine the elasticity of the DNA duplex in the native and stretched states, from the slopes of the force–distance curve (Figure 6). Before the structural transition, the estimated elastic constant of the LT–LS duplex was 0.20 ± 0.04 N/m. Assuming that DNA can be modeled as a uniform elastic rod, this value corresponds to an elastic modulus of 2.9×10^8 Pa. This number is in excellent agreement with the value of $(3.5 \pm 0.3) \times 10^8$ Pa calculated from the stretching data obtained on duplex DNA 15 μm in length [13], although it is not clear *a priori* that a short duplex should behave as a continuum object. After the structural transformation, the calculated elastic modulus increased sevenfold to 2.0×10^9 Pa; that is, the duplex became significantly stiffer. To our knowledge, the modulus in the stretched form of DNA has not been determined previously. The increased stiffness for the stretched duplex is likely to be due to stretching of bond angles in the phosphate backbone and hydrogen bonds between base pairs, whereas the elasticity of unstretched B-DNA is dominated by changes in dihedral angles and base tilting.

Significance

Highly specific interaction forces in double-stranded DNA are central to the storage and retrieval of genetic information. In addition, these forces determine the elastic properties of duplex DNA and are therefore critical for its packaging in the nucleus, cell division and many of its interactions with proteins. To date, much of our knowledge of these forces comes indirectly from measurements of binding energetics and structural data. But recent technological advances now enable the direct assessment of interaction and deformation forces at the single-molecule level in DNA and other biological systems. In this study, we describe direct measurements of the elongation and binding forces of individual DNA duplexes using chemical force microscopy, a relatively new technique that enables piconewton-resolution measurement of forces between molecules attached to a force microscope probe tip and a substrate. Mixed monolayers consisting of 14-mer oligonucleotides covalently linked to a hexadecanethiol and a 16-thiohexadecanol spacer were formed on gold-coated Si_3N_4 tips and silicon substrates to yield a low density of oligonucleotides protruding from a hydrophilic hydroxyl-terminated surface. The surface density ensured that at most one or two duplexes formed when the tip contacted the substrate. Separation forces between complementary oligonucleotide strands were found to be significantly larger than the forces measured between noncomplementary strands and were consistent with the unbinding of a single duplex. With increasing applied force, the separation of complementary strands proceeded in a stepwise manner, with B-form DNA straightened then structurally transformed to a stable stretched form of DNA approximately twice the length of the B-form and finally separated into single-stranded oligonucleotides. Thus, our data provide a direct measurement of the forces required to elastically deform and separate well-defined synthetic duplexes into single-stranded oligonucleotides.

DNA-binding proteins are known in many cases to stretch and bend the duplex structure. For example, when RecA binds to DNA there is an increase in the DNA length remarkably close to that observed for the stretched state of DNA. The work of strand deformation is clearly important to the function of this and other proteins. In the past, much effort has been devoted to recognizing and understanding the sequence specificity of binding by proteins, but it is worth considering how specific sequences also affect the energetics and mechanics of the initiation of transcription or repair. We believe that the approach outlined above offers a unique opportunity to address these fundamental biological issues. Chemical synthesis can now be exploited to prepare designed oligonucleotide sequences and force microscopy can be used to address directly the effects of specific sequences on the forces and energetics needed to deform and separate DNA duplexes in the absence or presence of DNA-binding proteins and molecules.

Materials and methods

Materials

All materials were of reagent grade and thoroughly dried by standard techniques. Water was deionized with a Barnstead NANOpure II filtration unit to 18 MΩ-cm resistivity.

Synthesis of $SH(CH_2)_{16}O$-oligonucleotides

2.05 g (7.93×10^{-3} moles) of $HO(CH_2)_{16}OH$ was placed in a 100 ml round bottom flask and 60 ml of CH_2Cl_2 added along with 0.05 equivalent of 4-dimethylaminopyridine (DMAP) and 1.4 equivalent of triethylamine and 0.695 ml of acetic anhydride. The reaction was monitored by thin layer chromatography (TLC) (silica gel, Kieselgel 60, EM Science; mobile phase 50:50 diethyl ether:hexane; cerium(IV) ammonium molybdate stain). The starting diol ($R_f = 0.05$) and diacetate ($R_f = 0.7$) were separated from the desired product (65% yield, $R_f = 0.25$) by flash chromatography (silica gel 60, EM Science; mobile phase 80:20 hexane:ether). The ^1H NMR, ^{13}C NMR and mass spectrum were consistent with the expected product.

0.5 g (1.7×10^{-3} moles) of the monoacetate protected diol [$HO(CH_2)_{16}OCH_3$] was slurried in 25 ml of dry pyridine and cooled to 4°C. TsCl (1 molar excess, 634 mg) was added with stirring and the reaction allowed to proceed for 36 h at 4°C and an additional 2 h at room temperature. The solution was poured into a beaker containing 200 ml of ice water with stirring and was then filtered. The recovered solid was

washed with water, dissolved in petroleum ether and charcoal was added. After filtration, the solution was evaporated to dryness. TLC revealed the desired product ($R_f = 0.58$) and the material purified by flash chromatography. The ^1H NMR, ^{13}C NMR and mass spectrum were consistent with the expected product.

0.37 g (8.1×10^{-4} moles) of the tosylated material [Ts-O$(CH_2)_{16}$ OCH_3] was dissolved in 10 ml of N,N'-dimethylformamide (DMF) and thoroughly degassed on a vacuum line. 1.1 equivalent of triphenylmethylmercaptan (TPMM, Aldrich) was dissolved in 5 ml of previously degassed ethanol. NaOH (1.05 equivalent) was dissolved in 150 µl of water and added via a syringe to the TPMM solution. This solution was cannulated into the DMF solution under positive pressure Argon. The reaction was allowed to proceed for 12 h and TLC revealed two products: $R_f = 0.4$ and 0.84. The materials were confirmed to the desired product ($R_f = 0.84$) and the product without the acetate protecting group ($R_f = 0.4$). The deacylated material [TrS$(CH_2)_{16}$OH] was purified by flash chromatography (80:20 hexane:diethyl ether) and dried thoroughly. The ^1H NMR, ^{13}C NMR and mass spectrum were consistent with the expected product.

220 mg (4.4×10^{-4} moles) of [TrS$(CH_2)_{16}$OH] was slurried in 15 ml of dry CH_2Cl_2 and 325 µl of N,N-diisopropylethylamine (DIEA) was added. 145 µl of 2-cyanoethyl-N,N-diisopropylchlorophosphoramidite was added dropwise via a syringe over 5 min. The reaction was allowed to proceed for 30 min and an additional 50 µl of the phosphoramidite was added. TLC (mobile phase: 50:50:1, hexane:diethyl ether:triethylamine) revealed the desired product $R_f = 0.72$ (ninhydrin stain). The material was purified by flash chromatography (mobile phase: 90:10:0.5). The isolated material was dried carefully, dissolved in dry acetonitrile and placed on an ABI automated DNA synthesizer. The coupling time for the modified nucleoside was increased to 30 min. Mass spectral analysis of the purified material revealed the expected parent ion ($M^+ = 4634$ calculated; 4634 found).

^{32}P labeling of oligonucleotides

Unmodified oligonucleotides for ^{32}P labeling were synthesized using standard solid phase techniques. LS, 5'-TCTGCATTGTCCGA-3', and LT, 5'-TCGGACAATGCAGA-3', were labeled using ^{32}P γ-ATP and T4 polynucleotide kinase by standard procedures. ^{32}P experiments were carried out using 1 pmol of DNA in 50 µl hybridization solution. Counts were measured on a Beckman Model LS-1801 scintillation counter.

Fluorescein labeling of oligonucleotides

Fluorescent oligonucleotides were synthesized using standard solid phase techniques by incorporating a linker fluorescein phosphoramidite (Glen Research) at the 5' ends. The 5'-fluorescein-TCTGCATTGTCCGA (LS) and 5'-fluorescein-TCGGACAATGCAGA (LT) oligonucleotides were purified by HPLC employing a C-18 reverse-phase column. A gradient of 2–40% CH_3CN and 0.1 M triethylammonium acetate (pH = 6.5) was used as the mobile phase. Fluorescence hybridization experiments were performed using 10 nmol of DNA in 50 µl of solution. Surface fluorescence was detected using a BioRad confocal microscope.

Hybridization of labeled oligonucleotides

All hybridization experiments were performed in 6 × SSC (saline sodium citrate: 0.9 M NaCl, 0.09 M sodium citrate, pH = 7, 6 ×) at 37°C overnight. After hybridization the sample was washed three times with 3 × SSC buffer at room temperature for 10 min each and once with 6 × SSC at 40°C for 30 min.

Gold-coated substrates and probe tips

Silicon (100) wafers (Silicon Sense, Nashua, NH; test grade, 525 µm thick) and commercial Si_3N_4 tip cantilever assemblies (Digital Instruments, Santa Barbara, CA, USA) were coated in an electron beam evaporator (base pressure 1×10^{-7} torr) with a 20 Å adhesion layer of titanium followed by 1000 Å of gold deposited at 1.5 Å/s. Silicon wafers were then cut into 2 cm × 2 cm square pieces and derivatized as described below.

Gold surface modification

A mixture of 1 µM LT or LS and 50–500 µM 16-thiohexadecanol in 50 mM triethylammonium acetate (pH 7.0) containing 25% ethanol was applied to the gold surface. 20 µl were applied in each experiment. By carefully applying the solution with a pipette tip, the volume covered a 1.5 cm diameter circle. The sample was incubated overnight at room temperature in a humid chamber. The samples were rinsed with 1:3 ethanol:H_2O and then with H_2O.

Chemical force microscopy

Force-displacement measurements were made with a Digital Instruments Nanoscope III Multi-Mode scanning force microscope equipped with a fluid cell. Modified tips were rinsed in water/ethanol mixture and dried under N_2 just prior to mounting them in the fluid cell. All measurements were done in 6 × SSC buffer. Normal spring constants of triangular 220 µm and 110 µm long Si_3N_4 cantilevers were determined using a nondestructive thermal resonance calibration method [33] and on average were 0.11 ± 0.01 N/m and 0.36 ± 0.02 N/m, respectively. High-resolution scanning electron microscope images were used to determine the tip radii after experiments and to verify the intactness of the tip coating. All the tips used for this study had radii of the order of 30–40 nm. All force versus distance curves were captured using Nanoscope III software and later analyzed on a Macintosh computer using a set of custom procedures written for Igor Pro 2.04 data analysis software (WaveMetrics Inc., Lake Oswego, OR, USA). Average binding force values were determined from histograms of the values obtained from at least 200 individual force versus displacement curves.

Acknowledgements

CML acknowledges partial support of this work by the Air Force Office of Scientific Research. TJM acknowledges partial support of this work by the Jet Propulsion Laboratory. TJM and JFK thank Yitzhak Tor and Scott Fraser for helpful discussions. AN thanks Leonid Mirny for helpful discussions and R. Lavery for providing coordinates for a model of stretched DNA.

References

1. Alberts, B., Bray, D., Lewis, J., Raff, M., Roberts, K. & Watson, J.D. (1994). *Molecular Biology of the Cell.* (3rd edn), Garland Publishing Inc., New York.
2. Austin, R., Brody, J., Cox, E., Duke, T. & Volkmuth, W. (1997). Stretch genes. *Physics Today* **50**, 32-38.
3. West, S. (1992). Enzymes and molecular mechanisms of genetic recombination. *Ann. Rev. Biochem.* **61**, 603-640.
4. Nicklas, R. (1988). The forces that move chromosomes in mitosis. *Annu. Rev. Biophys. Chem.* **17**, 431-449.
5. Erie, D., Yang, G., Schultz, H. & Bustamante, C. (1994). DNA bending by CRO protein in specific and nonspecific complexes: implications for protein site recognition and specificity. *Science* **266**, 1562-1566.
6. Klebe, G. & Bohm, H. (1997). Energetic and entropic factors determining binding affinity in protein-ligand complexes. *J. Recept. Signal Transduct. Res.* **17**, 459-473.
7. Marky, L.A. & Breslauer, K.J. (1987). Calculating thermodynamic data for transition of any molecularity from equilibrium melting curves. *Biopolymers* **26**, 1601-1619.
8. Turner, D. (1996). Thermodynamics of base pairing. *Curr. Opin. Struct. Biol.* **6**, 299-304.
9. Breslauer, K., Frank, R., Blocker, H. & Marky, L. (1986). Predicting DNA duplex stability from the base sequence. *Proc. Natl Acad. Sci. USA* **83**, 3746-3750.
10. Creighton, T.E. (1993). *Proteins: Structure and Molecular Properties.* (2nd edn), W.H. Freeman, New York.
11. Bensimon, D. (1996). Force: a new structural control parameter. *Structure* **4**, 885-889.
12. Cluzel, P., Lebrun, A., Heller, C., Lavery, R., Viovy, J.-L. & Chatenay, D. (1996). DNA: an extensible molecule. *Science* **271**, 792-794.
13. Smith, S.B., Cui, Y. & Bustamante, C. (1996). Overstretching B-DNA: the elastic response of individual double-stranded and single-stranded DNA molecules. *Science* **271**, 795-799.
14. Moy, V.T., Florin, E.L. & Gaub, H.E. (1994). Intermolecular forces and energies between ligands and receptors. *Science* **266**, 257-259.
15. Ashkin, A., Dziedzic, J.M., Bjorkholm, J.E. & Chu, S. (1986). Observation of a single-beam gradient force optical trap for dielectric particles. *Optics Lett.* **11**, 288-290.

16. Perkins, T., Smith, D.E. & Chu, S. (1994). Direct observation of tube-like motion of a single polymer chain. *Science* **264**, 819-822.
17. Marco, J.F. & Siggia, E.D. (1995). Stretching DNA. *Macromolecules* **28**, 8759-8770.
18. Smith, S., Finzi, L. & Bustamante, C. (1992). Direct mechanical measurement of the elasticity of single DNA molecules by using magnetic beads. *Science* **258**, 1122-1126.
19. Binnig, G., Quate, C.F. & Gerber, C. (1986). Atomic force microscope. *Phys. Rev. Lett.* **56**, 930-933.
20. Frommer, J. (1992). Scanning tunneling microscopy and atomic force microscopy in organic chemistry. *Angew. Chem., Int. Ed. Engl.* **31**, 1298-1328.
21. Shao, Z. & Yang, J. (1995). Progress in high resolution atomic force microscopy in biology. *Quart. Rev. Biophys.* **28**, 195-251.
22. Florin, E.L., Moy, V.T. & Gaub, H.E. (1994). Adhesion forces between individual ligand-receptor pairs. *Science* **264**, 415-417.
23. Lee, G.U., Kidwell, D.A. & Colton, R.J. (1994). Sensing discrete streptavidin-biotin interactions with atomic force microscopy. *Langmuir* **10**, 354-357.
24. Lee, G.U., Chrisey, L.A. & Colton, R.J. (1994). Direct measurement of the forces between complementary strands of DNA. *Science* **266**, 771-773.
25. Ulman, A. (1991). *Introduction to Ultrathin Organic Films*. Academic Press, New York.
26. Frisbie, C.D., Rozsnyai, L.F., Noy, A., Wrighton, M.S. & Lieber, C.M. (1994). Functional group imaging by chemical force microscopy. *Science* **265** , 2071-2074.
27. Noy, A., Frisbie, C.D., Rosznyai, L.F., Wrighton, M.S. & Lieber, C.M. (1995). Chemical force microscopy: exploiting chemically-modified tips to quantify adhesion, friction and functional group distributions in molecular assemblies. *J. Am. Chem. Soc.* **117**, 7943-7951.
28. Vezenov, D.V., Noy, A., Rosznyai, L.F. & Lieber, C.M. (1997). Force titrations and ionization-state sensitive imaging of functional groups in aqueous solutions by chemical force microscopy. *J. Am. Chem. Soc.* **119**, 2006-2015.
29. Nuzzo, R.G. & Allara, D.L. (1983). Adsorption of bifunctional organic disulfides on gold surfaces. *J. Am. Chem. Soc.* **105**, 4481-4483.
30. Bain, C.D., Troughton, E.B., Tao, Y.-T., Evall, J., Whitesides, G.M. & Nuzzo, R.G. (1989). Formation of monolayer films by the spontaneous assembly of organic thiols from solution onto gold. *J. Am. Chem. Soc.* **111**, 321-335.
31. Bain, C.D., Evall, J. & Whitesides, G.M. (1989). Formation of monolayers by coadsorption of thiols on gold: variations in head group, tail group and solvent. *J. Am. Chem. Soc* **111**, 7155-7164.
32. Whitesides, G.M. & Laibinis, P.E. (1990). Wet chemical approaches to characterization of organic surfaces: self-assembled monolayers, wetting and the physical organic chemistry of the solid-liquid interface. *Langmuir* **6**, 87-96.
33. Hutter, J.L. & Bechhoefer, J. (1993). Calibration of atomic-force microscope tips. *Rev. Sci. Instr.* **64**, 1868-1873.
34. Rao, B., Jwang, B. & Radding, C. (1990). RecA protein reinitiates strand exchange on isolated protein-free DNA intermediates. An ADP-resistant process. *J. Mol. Biol.* **213**, 789-809.
35. Lebrun, A. & Lavery, R. (1996). Modelling extreme stretching of DNA. *Nucleic Acid Res.* **24**, 2260-2267.
36. Bensimon, D., Simon, A.J., Croquette, V. & Bensimon, A. (1995). Stretching DNA with a receding meniscus: experiments and models. *Phys. Rev. Lett.* **74**, 4754-4757.
37. Thundat, T., Allison, D.P. & Warmack, R.J. (1994). Stretched DNA structures observed with atomic force microscopy. *Nucleic Acid Res.* **22**, 4224-4228.
38. Konrad, M.W. & Bolonick, J.I. (1996). Molecular dynamics simulation of DNA stretching is consistent with the tension observed for extension and strand separation and predicts a novel ladder structure. *J. Am. Chem. Soc.* **118**, 10989-10994.